ISSN 0023-1584, Kinetics and Catalysis, 2011, Vol. 52, No. 3, pp. 427–433. © Pleiades Publishing, Ltd., 2011.
Original Russian Text © A.V. Vosmerikov, V.I. Zaikovskii, L.L. Korobitsyna, V.V. Kozlov, N.V. Arbuzova, S.P. Zhuravkov, 2011, published in Kinetika i Kataliz, 2011, Vol. 52, No. 3, pp. 438–444.

Methane Conversion into Aromatic Hydrocarbons over Ag–Mo/ZSM-5 Catalysts

A. V. Vosmerikov[a], V. I. Zaikovskii[b], L. L. Korobitsyna[a], V. V. Kozlov[a], N. V. Arbuzova[a], and S. P. Zhuravkov[c]

[a] *Institute of Petroleum Chemistry, Siberian Branch, Russian Academy of Sciences, Tomsk, 634055 Russia*
[b] *Boreskov Institute of Catalysis, Siberian Branch, Russian Academy of Sciences, Novosibirsk, 630090 Russia*
[c] *Research Institute of High Voltages, Tomsk Polytechnic University, Tomsk, 634028 Russia*
e-mail: pika@ipc.tsc.ru

Received June 8, 2010

Abstract—Nonoxidative methane conversion into aromatic hydrocarbons over ZSM-5-type high-silica zeolites modified with nanosized powders of molybdenum (4.0 wt %) and silver (0.1–0.5 wt %) is reported. The acidic properties of the catalysts have been investigated by temperature-programmed ammonia desorption. The microstructure and composition of the Ag–Mo/ZSM-5 catalytic systems have been studied by high-resolution transmission electron microscopy and energy-dispersive X-ray spectroscopy. The doping of the Mo-containing zeolite with silver enhances its activity and stability in nonoxidative methane conversion into aromatic hydrocarbons.

DOI: 10.1134/S0023158411030190

Natural and associated gases are important potential hydrocarbon stocks for the synthesis of various valuable chemicals, including products that are currently obtained from petroleum. In order to establish the scientific foundations of this synthesis, it is necessary to profoundly investigate and develop the conversion routes of methane, the most abundant and most stable component of these stocks. Of particular interest is the one-step catalytic synthesis of aromatic compounds from methane under nonoxidative conditions over ZSM-type high-silica zeolites modified with transition metal ions. The most comprehensively studied zeolite systems are those containing Mo and W [1–3]. A significant drawback of these catalysts is their rapid deactivation under the severe conditions of the process. The stable service life of Mo- and W-containing pentasils is extended in various ways, including the introduction of various metals: Y, Cu, Zr, La, Pt, and Fe [4–7].

Here, we report the effect of silver on the acidic and catalytic properties of the Mo/ZSM-5 system in the nonoxidative conversion of methane into aromatic hydrocarbons. Using high-resolution transmission electron microscopy (HRTEM) and energy-dispersive X-ray (EDX) spectroscopy, we studied the nature and distribution of active sites and the structure of carbon-containing deposits forming on the surface of Ag–Mo/ZSM-5 catalysts at different on-stream times.

EXPERIMENTAL

Catalysts were prepared by dry mixing of a ZSM-5-type zeolite ($SiO_2 : Al_2O_3 = 50$ mol/mol) with Mo and Ag nanopowders. The zeolite was obtained by hydrothermal crystallization using carbamide as the structure-forming agent [8]. The Mo and Ag nanopowders were produced by electric blasting of a wire in argon [9]. The Mo/ZSM-5 catalyst, prepared by the mechanical mixing of the zeolite and Mo nanopowder in a KM-1 vibratory ball mill, was calcined at 540°C for 6 h. The Mo content of the catalyst was 4.0 wt %. Ag–Mo/ZSM-5 samples were obtained by adding Ag nanopowder to the (4.0% Mo)/ZSM-5 catalyst. The silver content of the catalytic system was varied between 0.05 and 2.0 wt %. The Ag–Mo/ZSM-5 catalysts prepared by mechanical mixing were not calcined.

The nonoxidative conversion of methane (99.9%) was carried out in a flow reactor at 700–750°C, GHSV = 1000 h^{-1}, and atmospheric pressure. The products of the reaction were analyzed by gas chromatography. Catalyst testing in methane dehydroaromatization is detailed in our earlier work [10].

The acidic properties of the catalysts were studied by temperature-programmed desorption of ammonia, which enabled us to determine the acid site strength distribution and concentration.

HRTEM images were obtained on a JEM 2010 microscope (JEOL) with a lattice resolution of 0.14 nm at an accelerating voltage of 200 kV. The specimens to be examined by HRTEM were prepared on a holey carbon support secured on a copper grid. The high-resolution images of periodic structures were analyzed using the Fourier method.

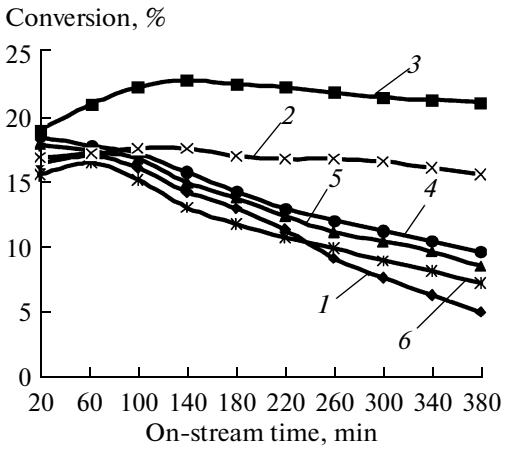

Fig. 1. Methane conversion as a function of the catalyst on-stream time: (*1*) initial (4.0% Mo)/ZSM-5; (*2–6*) the same catalyst containing (*2*) 0.05, (*3*) 0.1, (*4*) 0.5, (*5*) 1.0, and (*6*) 2.0% Ag nanopowder (750°C, GHSV = 1000 h^{-1}).

Local elemental analyses were carried out by EDX spectroscopy on an EDAX spectrometer (EDAX Co.) equipped with a Si(Li) detector with an energy resolution of 130 eV or higher.

RESULTS AND DISCUSSION

Figure 1 shows how the methane conversion at 750°C depends on the Ag nanopowder content of the (4.0% Mo)/ZSM-5 catalyst and on the on-stream time. The most active and most stable catalyst is (4.0% Mo)/ZSM-5 containing 0.1% Ag: the methane conversion remains fairly high over a long testing time and exceeds 20% after 380-min-long operation. As the on-stream time is further increased, the activity of this catalyst gradually declines, and after 720 min the methane conversion is 7.4%. As the Ag nanopowder content of the (4.0% Mo)/ZSM-5 catalyst is raised from 0.5 to 2.0%, the activity and stability of the catalyst decrease. The methane conversion over (2.0% Ag–4.0% Mo)/ZSM-5 after 380 min is 7.3%, three times lower than is observed for the catalyst containing 0.1% Ag. It is likely that, as the silver concentration in the catalytic system is increased, the degree of dispersion of silver changes because of particle agglomeration during the reaction. This leads to the blocking of active Mo_2C surface sites and zeolite channels, in which the molybdenum oxide-like clusters and intrinsic acid sites of the zeolite are located [11]. The HRTEM and EDX data presented below confirm the presence of Ag in molybdenum carbide particles and Ag as micron-sized aggregates.

As the temperature is lowered to 700°C, the stable service life of the catalyst lengthens markedly and the methane conversion remains rather high. Over the initial 380 min of the reaction, the activity of the (0.1% Ag–4.0% Mo)/ZSM-5 catalyst at 700°C is somewhat lower than at 750°C, but thereafter it is higher over a long time: the methane conversion after 720 min is 14.9% at 700°C and only 7.4% at 750°C. The catalyst is fairly active after 2040-min-long (34-h) operation as well, ensuring 12.6% conversion.

Table 1 lists the percentages of the main products of methane conversion on Mo/ZSM-5 catalysts with different Ag nanopowder contents. Clearly, the ethane and ethylene concentrations gradually increase during the reaction, but the total yield of these hydrocarbons does not exceed 0.8%.

Analysis of the liquid products of methane conversion demonstrated that the highest benzene yield is attained with the (0.1% Ag–4.0% Mo)/ZSM-5 catalyst. During the reaction, the benzene concentration gradually decreases and the benzene : naphthalene ratio varies in a wide range. For all of the bimetallic zeolite-supported catalysts, the naphthalene yield is much higher than the benzene yield. The largest amount of naphthalene forms over the (0.1% Ag–4.0% Mo)/ZSM-5 catalyst, with the benzene : naphthalene ratio changing from 0.56 to 0.38 throughout the on-stream time. Thus, the introduction of silver nanopowder into the Mo-containing zeolite does not change the qualitative composition of the methane conversion products, but alters the component ratios in the gas and liquid phases, which depend on the Ag content of the catalyst.

Thus, our study demonstrated that the introduction of 0.05–0.1% Ag nanopowder into the (4.0% Mo)/ZSM-5 catalyst markedly enhances its activity and time-on-stream stability in methane conversion into aromatic hydrocarbons.

In view of the bifunctional action of the catalysts, which is due to the involvement of both Mo-containing active sites and intrinsic Brønsted acid sites of the zeolite, it is interesting to consider the acidic properties of the high-silica zeolite used in catalyst preparation and those of its molybdenum- and silver-modified forms. Our data characterizing the acidic properties of the catalysts are presented in Table 2.

The Mo nanopowder introduced into zeolite ZSM-5 reduces the strength and concentration of its acid sites: the total acid site concentration decreases from 940 to 632 μmol/g, and the concentration of high-temperature sites, which are conventionally viewed as Brønsted acid sites, decreases from 416 to 204 μmol/g. These changes in the acidic properties of the zeolite are due to the fact that, during the calcination of the catalyst as a part of its preparation procedure, the Brønsted acid sites interact with Mo species to yield $Al_2(MoO_4)_3$, an inactive phase. The addition of 0.1 Ag nanopowder to the (4.0% Mo)/ZSM-5 catalyst does not exert any significant effect on the strength and concentration of its acid sites. This is likely due to the fact that, after the addition of Ag, the catalyst was not calcined and, as a consequence, the dopant did not interact with the zeolite matrix or Mo species. This assumption is proved by electron microscopy data.

Table 1. Effect of the Ag nanopowder content of the (4.0% Mo)/ZSM-5 catalyst on the yields of methane conversion products (750°C)

Ag, wt %	On-stream time, min									
	20	60	100	140	180	220	260	300	340	380
C_2H_6 yield, %										
–	0.04	0.07	0.09	0.11	0.12	0.13	0.13	0.13	0.14	0.11
0.05	0.04	0.07	0.10	0.13	0.13	0.13	0.13	0.14	0.16	0.18
0.1	0.01	0.05	0.10	0.15	0.16	0.16	0.16	0.18	0.20	0.17
0.5	0.04	0.06	0.06	0.07	0.11	0.12	0.14	0.14	0.14	0.09
1.0	0.06	0.06	0.06	0.10	0.11	0.12	0.15	0.12	0.11	0.09
2.0	0.03	0.06	0.06	0.09	0.11	0.09	0.08	0.06	0.04	0.03
C_2H_4 yield, %										
–	0.07	0.13	0.18	0.21	0.23	0.29	0.34	0.40	0.49	0.55
0.05	0.04	0.11	0.12	0.13	0.17	0.19	0.23	0.26	0.27	0.31
0.1	0.01	0.04	0.05	0.06	0.06	0.07	0.10	0.14	0.15	0.18
0.5	0.09	0.14	0.19	0.22	0.30	0.36	0.42	0.45	0.59	0.71
1.0	0.19	0.16	0.23	0.30	0.36	0.43	0.51	0.59	0.67	0.72
2.0	0.18	0.19	0.31	0.38	0.50	0.63	0.67	0.68	0.71	0.76
C_6H_6 yield, %										
–	5.56	5.71	4.98	4.89	4.45	4.24	3.89	3.20	2.70	2.36
0.05	4.79	5.89	6.25	5.91	5.44	5.22	5.02	4.68	4.31	4.12
0.1	4.83	5.99	6.33	6.31	5.98	5.89	5.54	5.36	4.95	4.24
0.5	5.63	5.79	5.01	4.76	3.99	3.43	3.33	2.85	2.55	1.42
1.0	5.58	5.61	4.69	4.10	3.50	3.09	2.56	2.23	1.73	1.22
2.0	5.37	5.07	4.22	3.87	2.90	2.38	1.93	1.62	1.10	1.00
$C_{10}H_8$ yield, %										
–	8.20	7.68	6.81	6.20	5.97	4.66	2.98	2.49	1.82	1.54
0.05	6.52	7.03	7.46	7.66	7.78	7.87	8.02	8.24	8.11	7.88
0.1	9.53	10.63	11.63	11.70	11.76	11.78	11.68	11.66	11.58	11.22
0.5	9.06	8.25	7.86	7.19	6.89	6.33	5.59	4.43	2.96	2.14
1.0	8.54	8.00	6.83	5.99	5.84	5.30	5.16	3.85	2.49	1.34
2.0	7.96	7.84	6.64	5.13	5.06	4.87	4.19	3.75	1.14	0.98

Electron microscopic examinations showed that the fresh (0.1% Ag–4.0% Mo)/ZSM-5 sample is dominated by zeolite particles and contains silver particles as micron-sized aggregates (Fig. 2a). The arrangement of the zeolite and silver particles indicates no topochemical interactions between them. No separate particles of molybdenum compounds were observed in the sample. Only in a few cases does the zeolite surface have higher contrast particles assignable to a molybdenum compound according to EDX data. At the same time, the EDX spectra from zeolite areas containing no particles show the Mo signal, suggesting that the zeolite contains oxidized molecular molybdenum species (Fig. 2c).

For the (0.1% Ag–4.0% Mo)/ZSM-5 sample that has been on stream for 10 min in methane dehydroar-

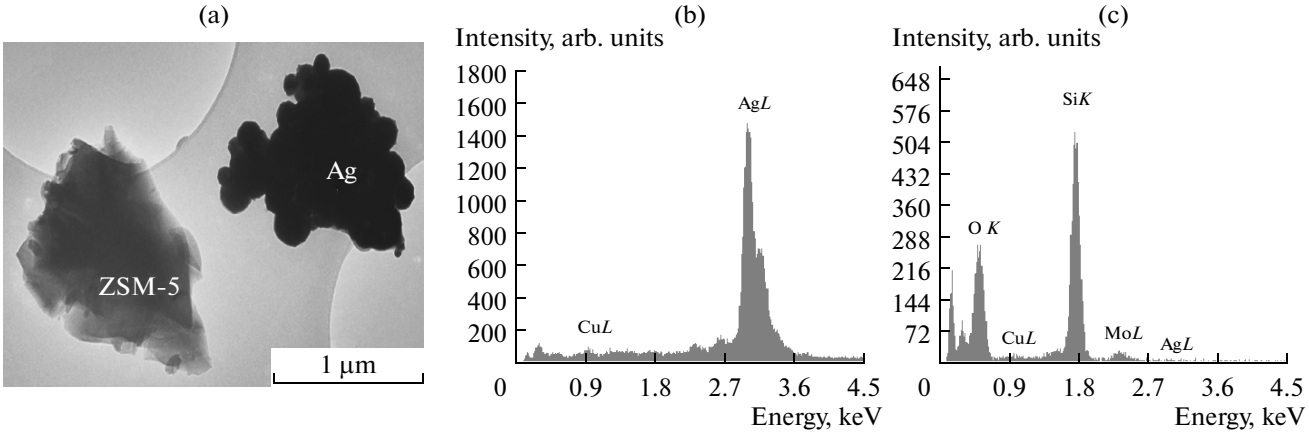

Fig. 2. (a) HRTEM image of zeolite and silver particles of the fresh (0.1% Ag–4.0% Mo)/ZSM-5 catalyst. (b, c) EDX spectra of (b) silver and (c) zeolite particles in this catalyst.

omatization at 750°C, the supported component is typically dispersed on the zeolite surface in the form of molybdenum carbide (Fig. 3a). The size of the molybdenum carbide particles is 5–10 nm, but aggregation into agglomerates up to 50 nm in size is typical of the primary crystallites. The molybdenum carbide particle surface shows only thin graphene islands, which are mostly not thicker than two carbon monolayers (Fig. 3b).

The sample that has been on stream for 380 min in methane dehydroaromatization has many three-dimensional particles of Mo_2C in close contact with zeolite crystallites (Figs. 4, 5). The molybdenum carbide particles (5–50 nm) are faceted into an elongated or planer shape. The HRTEM image of the crystal lattice and the two-dimensional Fourier pattern illustrating the identification of molybdenum carbide based on its reflections are presented in Fig. 4b.

No individual silver particles were observed in the catalyst after the reaction. However, according to EDX data, silver is present in the molybdenum carbide particles located on the zeolite surface. Figure 5b shows the EDX spectrum indicating that the Ag : Mo atomic ratio in the Mo_2C particle is 6 : 94. A variety of binary compounds between Ag and Mo are known from the literature [12]. Apparently, the formation of the mixed compound (containing oxidized forms of the metals) takes place in the gas phase upon the 380-min-long heat treatment of the catalyst at 750°C during the reaction, as was observed earlier for catalysts containing Ni nanopowder [13]. The detection of silver in the surface Mo_2C particles is evidence that molybdenum carbide is doped with silver; according to EDX data, the composition of solid solution is $(Ag_{0.06}Mo_{0.94})_2C$. A comparison between the atomic ratio Ag : Mo = 6 : 94 and the total Ag and Mo contents of the catalyst indicates that part of the molybdenum is not incorporated in surface carbide particles of the Ag–Mo–C type. As in the case of the initial catalyst Mo/ZSM-5, the EDX spectrum recorded for the zeolite area containing no three-dimensional Mo_2C particles shows a signal from Mo (Fig. 5c). This is explained by the fact that a considerable part of the molybdenum is located in zeolite channels, existing in the form of oxide-like clusters, whose nature was studied by HRTEM and EPR spectroscopy in our earlier work [14]. At the same time, note that there is no sig-

Table 2. Acidic properties of catalysts

Catalyst	T_{max}, °C		Concentration, μmol/g		
	T_I	T_{II}	C_I	C_{II}	C
ZSM-5	190	420	524	416	940
4.0% Mo/ZSM-5	175	410	428	204	632
0.1% Ag–4.0% Mo/ZSM-5	175	410	420	200	620

Note: T_I and T_{II} are the temperature maxima of the low- and high-temperature peaks; C_I, C_{II}, and C are the concentrations of the low- and high-temperature acid sites and the total acid site concentration, respectively.

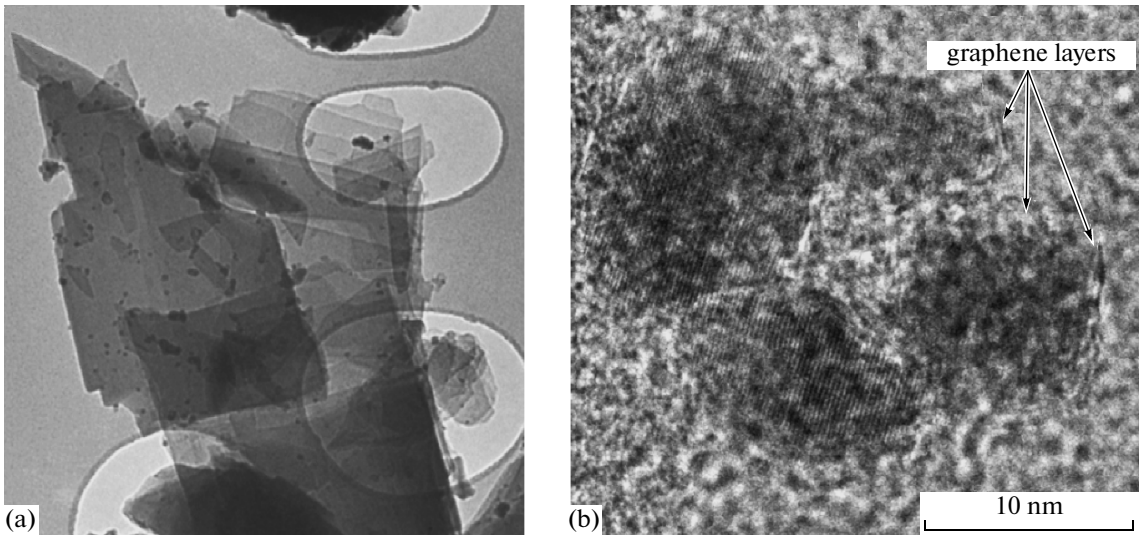

Fig. 3. HRTEM images of the (0.1% Ag–4.0% Mo)/ZSM-5 catalyst that has been on stream for 10 min in methane dehydroaromatization: (a) zeolite crystals with supported molybdenum carbide particles, (b) aggregated primary crystallites of molybdenum carbide with graphene layers on their surface (shown by arrows).

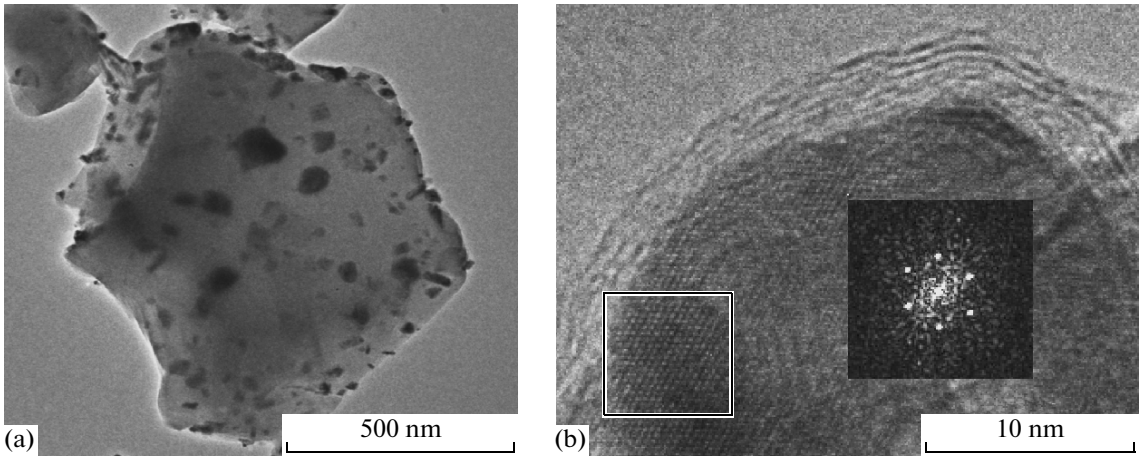

Fig. 4. (a) HRTEM image of the (0.1% Ag–4.0% Mo)/ZSM-5 catalyst that has been on stream for 380 min in methane dehydroaromatization; (b) graphite-like layers on the Mo_2C surface. The inset shows the Fourier pattern with reflections from Mo_2C ($d_{100} = 0.26$ nm, $d_{002} = 0.24$ nm, $d_{101} = 0.23$ nm) and the corresponding area of the image.

nal from Ag in these spectra and, therefore, the clusters contain no silver.

In the (0.1% Ag–4.0% Mo)/ZSM-5 sample after the reaction, there is a graphite-like carbon layer 2–4 nm in thickness on the surface of Mo_2C particles (Fig. 4b). Graphite-like islands also form on the zeolite surface, but these are not thicker than 1 nm (Fig. 5a). Thus, the zeolite surface and, therefore, the zeolite channels are coked much less strongly in the course of methane conversion than the surface of silver-doped molybdenum carbide. The carbon filaments present in the (Ni–Mo)/ZSM-5 catalyst after thermal treatment with methane [13] were not detected in (0.1% Ag–4.0% Mo)/ZSM-5.

The molybdenum carbide particles in the samples that have worked in methane dehydroaromatization over different periods of time have practically the same morphology. The only difference is that the primary particles coarsen to some extent (Figs. 6a, 6b). Carbon deposits up to ten graphene monolayers in thickness can be seen on the particle surfaces (Fig. 6c).

At the same time, part of the active component, Mo, is located in the zeolite channels in the form of clusters (~1 nm) [11]. Fig. 6d shows a large molybdenum carbide particle on the zeolite surface (object 1)

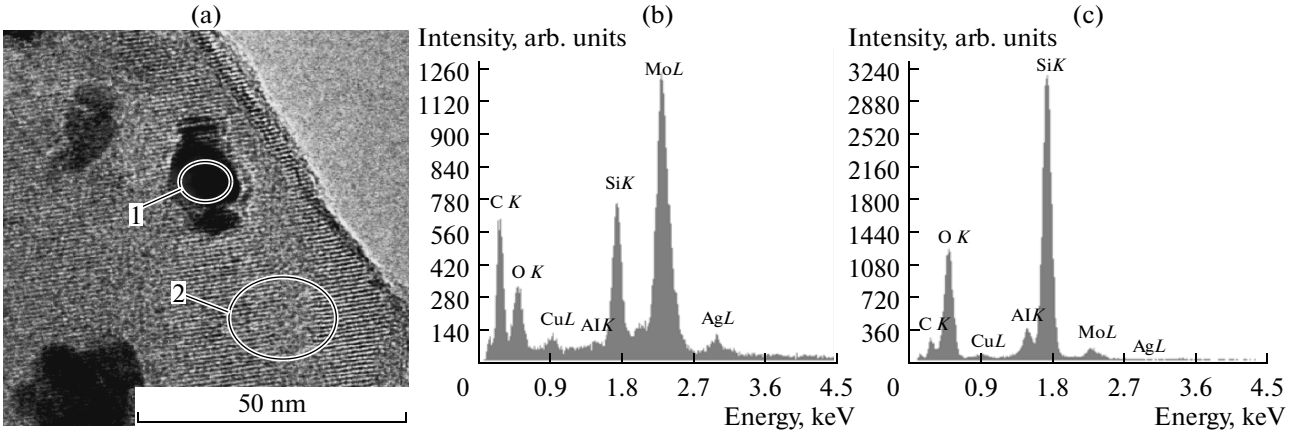

Fig. 5. (a) HRTEM image of the (0.1% Ag–4.0% Mo)/ZSM-5 catalyst that has been on stream for 380 min in methane dehydroaromatization, showing Mo_2C particles of different sizes (the circles indicate the areas analyzed by EDX spectroscopy). (b, c) EDX spectra of a Mo_2C particle (1) and a zeolite area without visible Mo_2C particles (2), respectively.

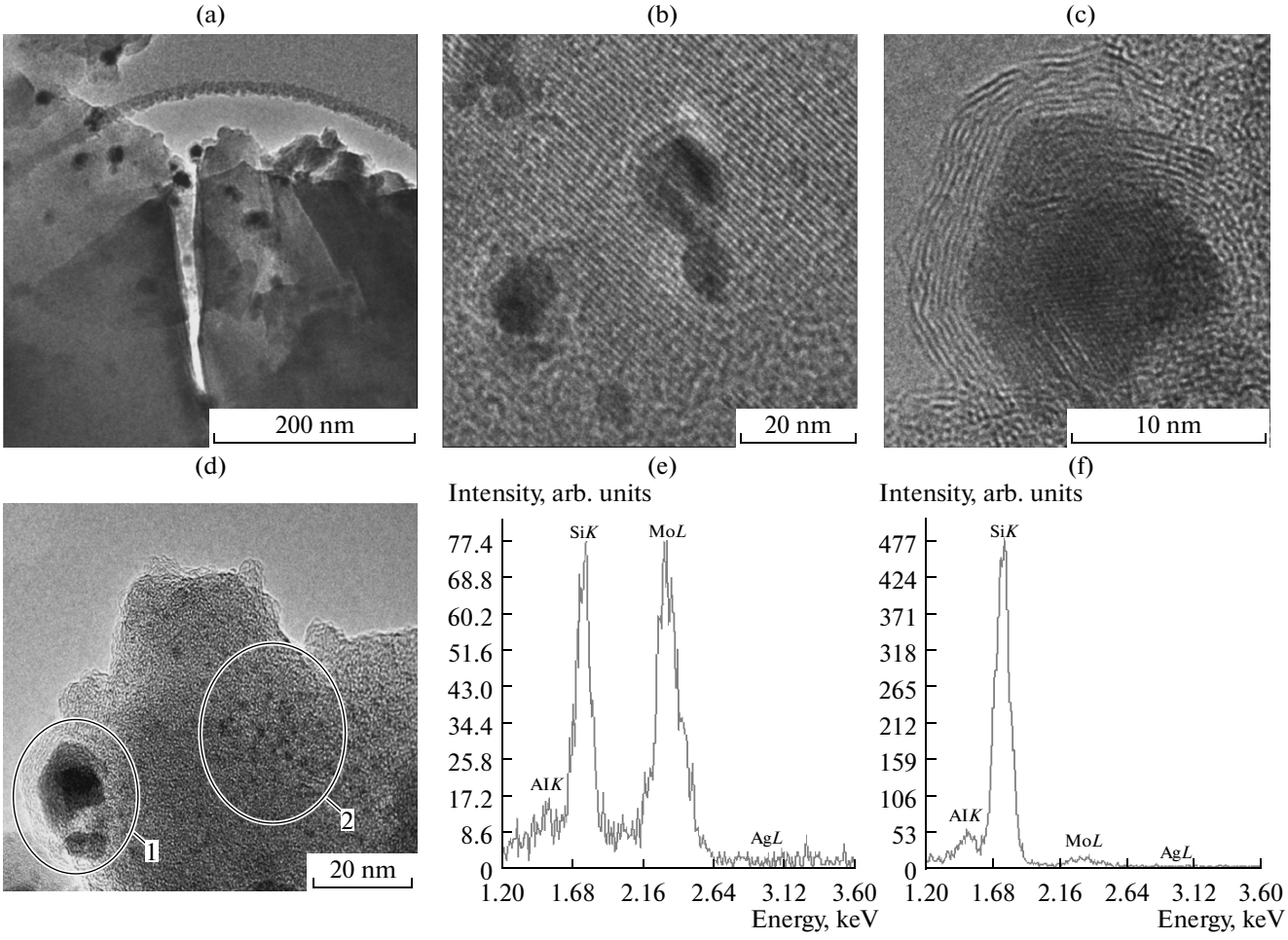

Fig. 6. (a–d) HRTEM images of the (0.1% Ag–4.0% Mo)/ZSM-5 catalyst that has been on stream for 2040 min in methane dehydroaromatization: (a, b) zeolite crystals with supported molybdenum carbide particles at different magnifications; (c) carbon deposit on the molybdenum carbide surface; (d) molybdenum carbide particle on the zeolite surface (1) and Mo clusters in the zeolite bulk (2). (e, f) EDX spectra of the zeolite areas circled in Fig. 6d: (e) 1 and (f) 2.

and an area with small particles (clusters) in the zeolite bulk (object 2). The presence of Mo in the zeolite bulk is confirmed by EDX spectra taken from these objects (Figs. 6e, 6f). Note that the EDX spectra of the (0.1% Ag–4.0% Mo)/ZSM-5 sample that has been on stream for 2040 min indicate no Ag traces both in the surface particles and in the clusters in the zeolite bulk. For the catalyst that has been on stream for 380 min, we found that silver is incorporated in the large molybdenum carbide particles located on the zeolite surface. Therefore, the long operation of the catalyst in methane dehydroaromatization removes silver from the molybdenum carbide particles.

Thus, the doping of the Mo/ZSM-5 catalyst with silver enhances its activity and extends its stable service life in methane dehydroaromatizaion. The highest activity and stability are shown by the Mo/ZSM-5 catalyst containing 0.1% Ag nanopowder. The longer stable service life of the silver-containing Mo/ZSM-5 catalyst is due to the decrease in the coking rate, which is particularly pronounced at lower reaction temperatures. Unlike the Ni- and Mo-containing zeolite [13], the Ag-containing catalyst yields no filamentous carbon, which might block zeolite pores at long on-stream times. It is likely due to this fact that the Mo/ZSM-5 system containing a small amount of silver shows a more stable performance.

ACKNOWLEDGMENTS

This work was supported by the Presidium of the Russian Academy of Sciences (grant no. 21-50).

REFERENCES

1. Xu, Y. and Lin, L., *Appl. Catal., A*, 1999, vol. 188, p. 53.
2. Shu, Y. and Ichikawa, M., *Catal. Today*, 2001, vol. 71, p. 55.
3. Zhou, T., Lui, A., Mo, Y., and Zhang, H., *J. Phys. Chem. A*, 2000, vol. 104, p. 4505.
4. Chen, L., Lin, L., and Xu, Z., *Catal. Lett.*, 1996, vol. 39, p. 169.
5. Wang, L., Xu, Y., Wong, S., Cui, W., and Guo, X., *Appl. Catal., A*, 1997, vol. 152, p. 173.
6. Liu, S., Dong, Q., Ohnishi, R., and Ichikawa, M., *Chem. Commun.*, 1997, p. 1445.
7. Wang, Q. and Lin, W., *J. Nat. Gas Chem.*, 2004, vol. 13, p. 91.
8. Korobitsyna, L.L. and Barbashin, Ya.E., in *Sintez na osnove produktov neftekhimii: Sbornik trudov* (Syntheses Based on Petrochemical Products: Collection of Works), Novosibirsk: Nauka, 1990, p. 314.
9. Gusev, A.I., *Nanokristallicheskie materialy: Metody polucheniya i svoistva* (Nanocrystalline Materials: Preparation and Properties), Yekaterinburg: Ural. Otd. Ross. Akad. Nauk SSSR, 1988, p. 199.
10. Vosmerikov, A.V., Echevskii, G.V., Korobitsyna, L.L., Barbashin, Ya.E., Arbuzova, N.V., Kodenev, E.G., and Zhuravkov, S.P., *Kinet. Katal.,* 2005, vol. 46, no. 5, p. 769 [*Kinet. Catal.* (Engl. Transl.), vol. 46, no. 5, p. 724].
11. Zaikovskii, V.I., Vosmerikov, A.V., Anufrienko, V.F., Korobitsyna, L.L., Kodenev, E.G., Echevskii, G.V., Vasenin, N.T., Zhuravkov, S.P., Ismagilov, Z.R., and Parmon, V.N., *Dokl. Akad. Nauk*, 2005, vol. 404, no. 4, p. 500 [*Dokl.* (Engl. Transl.), vol. 404, nos. 4–6, p. 201].
12. *Powder Diffraction File 2*, Swarthmore: Joint Committee on Powder Diffraction Standards, 1997, nos. 21-1342, 21-1340, 21-1339.
13. Vosmerikov, A.V., Zaikovskii, V.I., Korobitsyna, L.L., Echevskii, G.V., Kozlov, V.V., Barbashin, Ya.E., and Zhuravkov, S.P., *Kinet. Katal.*, 2009, vol. 50, no. 5, p. 755 [*Kinet. Catal.* (Engl. Transl.), vol. 50, no. 5, p. 725].
14. Zaikovskii, V.I., Vosmerikov, A.V., Anufrienko, V.F., Korobitsyna, L.L., Kodenev, E.G., Echevskii, G.V., Vasenin, N.T., Zhuravkov, S.P., Matus, E.V., Ismagilov, Z.R., and Parmon, V.N., *Kinet. Katal.*, 2006, vol. 47, no. 3, p. 396 [*Kinet. Catal.* (Engl. Transl.), vol. 47, no. 3, p. 389].